

Carbon Dioxide Emissions from Oil Shale Derived Liquid Fuels

Adam R. Brandt^{1,4}, Jeremy Boak², and Alan K. Burnham³

¹Energy and Resources Group, University of California, Berkeley CA 94024

²Center for Oil Shale Technology & Research, Colorado School of Mines,
Golden CO 80401

³American Shale Oil LLC, Rifle, CO 81650

⁴Current address: Department of Energy Resources Engineering, Stanford
University, Stanford CA 94305-2220
abrandt@stanford.edu

Without mitigation or technology improvements, full-fuel-cycle carbon dioxide (CO₂) emissions from oil shale derived liquid fuels are likely to be 25 to 75% higher than those from conventional liquid fuels, depending on the details of the process used. The emissions of CO₂ from oil shale derived fuels come from three stages: retorting of shale, upgrading and refining of raw shale oil, and combustion of the finished transportation fuels. Emissions from these stages represent approximately 25-40%, 5-15%, and 50-65% of total fuel-cycle emissions, respectively. The most uncertain source of emissions is the retorting stage, due to variation in emissions with shale quality and retorting technology used. Mitigation options include higher thermal efficiency, minimizing carbonate decomposition, CO₂ sequestration by geologic injection, enhanced oil recovery, mineralization in spent retorts, or the use of non-fossil sources for process heat.

Introduction – Carbon dioxide and oil shale

The world resource of oil shale likely consists of trillions of barrels of hydrocarbon (HC) product, with significant resources distributed worldwide (1). Both scientific investigation and production of oil shale resources have been episodic, coinciding with peaks in the price of oil. This is due to the high cost of oil production from shale. Recent oil price increases have driven a resurgence of interest in oil shale development around the world.

Current methods of producing HCs from oil shale involve mining and retorting shale at the surface to convert immature kerogen to liquids and gas (*ex situ* retorting). Common fuel sources for *ex situ* retorting are pyrolysis gas and “char,” a shale oil coke generated during the production of liquid HCs from kerogen. *In situ* conversion of kerogen to HCs holds promise, but a major increase in production is more than a decade away. Methods considered for *in situ* heating include borehole electrical heaters, electrical heating through fractures propped with conductive material, fluid heat transport through boreholes, and borehole-installed fuel cell heaters (2).

Given current concern about anthropogenic climate change, a major hurdle for production of fuels from oil shale is the quantity of carbon dioxide (CO₂) emitted from oil shale processing. Early analysis of this problem presented a very wide range of possible emissions consequences (3). Recent research attention has focused on this problem (4-10), but significant uncertainties remain. This chapter summarizes the state of knowledge regarding CO₂ emissions from oil shale retorting, and discusses the remaining uncertainties.

This chapter explores emissions from the full liquid fuel production cycle, and generally uses parameters derived from the Green River Formation (GRF) oil shale of the Western United States, the largest resource of oil shale in the world (1). This fuel cycle includes three stages: retorting raw shale to produce crude shale oil, upgrading and refining of crude shale oil, and combustion of the final refined fuel. Emissions from the first stage, oil shale retorting, are the most uncertain, and will be the primary focus of this chapter. Key sources of CO₂ from oil shale retorting include CO₂ generated by the breakdown of carbonate minerals, by the oxidation of kerogen during pyrolysis, by combustion of fuels to provide thermal energy for retorting, and by fossil fuel power plants used to generate electricity used in the retorting process. Emissions from the last two stages are less uncertain and will be described in less detail. Note that this chapter focuses solely on conversion of kerogen to liquid and gaseous HCs, and does not address the use of oil shale for power generation.

For the calculations presented in this chapter, energy requirements and CO₂ emissions are reported either per tonne (t) of raw shale processed, or per megajoule (MJ) of refined fuel delivered (RFD) to the end consumer. The refined fuel of comparison will be reformulated gasoline (U.S. Federal standard). We use the higher heating value (HHV) basis of fuels.

Sources of carbon dioxide from fuel production stages

Carbon dioxide is directly emitted in all three primary stages of producing and consuming fuels from oil shale. First are emissions resulting from the retorting of oil shales to generate unrefined hydrocarbons (HCs), including crude shale oil and HC gases. Second are emissions from the upgrading and refining of crude shale oil to refined fuels (e.g., gasoline or diesel). Third, direct emissions result from combustion of the refined fuel by the consumer. Additionally, there are minor indirect emissions from the consumption of materials such as steel or cement used in oil shale extraction.

Emissions from generating crude hydrocarbons through oil shale retorting

Emissions from oil shale retorting process can be divided into three components: CO₂ emitted due to the thermal energy requirements of retorting, CO₂ emitted from other energy uses associated with retorting, and CO₂ emitted from the shale itself. These emissions sources will be discussed in order.

Carbon dioxide emissions from thermal requirements for retorting

A major source of emissions is the thermal energy requirement for retorting. These thermal requirements can be met by direct combustion of fuels, or indirectly by combustion of fuels for electric power generation.

The thermal energy demands of retorting can be defined as the *heat of retorting*, which is an overall heat requirement that includes (11, p. 32):

- a) The heat content of shale mineral matter at final temperature of the retorted shale (which could be lower than the retorting temperature, as in the Paraho process where heat is recovered from spent shale);
- b) The heat of reaction of kerogen decomposition;
- c) The heat of reaction of mineral reactions in shale (e.g., decomposition of carbonates);
- d) The heat to vaporize generated hydrocarbons and water contained in shale (both bound and free water);

- e) The heat contents of gas, water, and oil vapors at the temperature of exit from the retort.

The heat of retorting varies with shale character and with the retorting technology used. Measured values vary significantly between samples and studies, and it is difficult to generalize about the heat of retorting (*12, p. 149*). Reported heats of retorting range from as low as 240 MJ/t to as high as 880 MJ/t across a variety of studies (*12, Table 8.10*). We will explore the reasons for this variability below.

Because of factors (a) and (e) above, the heat of retorting depends strongly on the rate at which heating takes place. This is because slower retorting results in lower temperatures of complete kerogen decomposition. At a heating rate of 0.5°C/day, kerogen will be effectively decomposed upon reaching 340-360°C, as compared to 500°C for the Fischer Assay at 12°C/min (FA – the standard process for measuring liquid content of oil shale). This 150°C temperature difference will result in an increase in the heat of retorting by 140 MJ/t from the slow to the fast process due solely to the change in enthalpy of the shale mineral matter (*13*).¹ Also with faster retorting, produced HCs leave as vapor at a higher temperature, which increases heat requirements by <10 MJ/t.²

The heat of retorting varies little with changes in the mineral composition of shale (*13*). Because the enthalpies of typical mineral components of GRF shale do not vary greatly, Camp (*13*) found that large shifts in the percentage composition of shale mineral matter were required to cause even a 1% change in the weighted heat capacity of the minerals (note that this excludes the effects of bound water and mineral decomposition, which can have large effects and are discussed below).

The above values for mineral matter are only strictly true in simple retorting systems with no heat recovery from spent shale. In retorts with beneficial heat recovery from the spent shale (e.g., the Alberta Taciuk Processor [ATP], a modern ex situ retort with countercurrent heat exchange), the net heat requirement depends on the temperature of the spent shale as it exits the retort. This does not include spent shale that is water cooled, unless the heat of the steam is used for a beneficial purpose.

Because of factor (b) above, the heat of retorting increases as the organic content of the shale increases. An increase in organic content corresponding to a

¹ These values do not account for decomposition of any saline or carbonate minerals, as these factors are discussed below.

² Camp (*13*) notes that the change in sensible heat of kerogen between 350 and 500 °C will be 50 kJ/kg of kerogen larger than that of the retort products if oil is in the vapor phase. Since the organic content of GRF shale is 16-20% for 110-150 l/t shale, this amounts to <10 MJ/t of shale processed.

yield increase from 20 to 200 l/t will increase the heat of retorting from ~600 to ~800 MJ/t (14). Mraw and Keweshan (15) found empirically that a 110 l/t Green River shale will have a heat of retorting of about 700 MJ/t, while a 150 l/t shale will require about 750 MJ/t.³ The richest shales studied (>300 l/t) have heats of retorting approaching 1000 MJ/t (15).

Because of factor (c) above, the heat of retorting varies with reactions involving shale mineral matter, including mineral dissociation and dehydration. Many of these reactions are endothermic, adding to the required energy inputs of retorting. Common reactions that occur in shale are shown in Table 1, numbered and grouped by species. Many of these reactions also result in release of inorganic CO₂, but here we are only concerned with their effects on the heat of retorting (see below for discussion of mineral CO₂ emissions).

The relevant mineral reactions can be grouped into reactions involving calcite (CaCO₃), dolomite (MgCa(CO₃)₂), sodium minerals, and pyrite (FeS₂). Reactions involving calcite, dolomite and sodium minerals are endothermic, and therefore add to the heat of retorting. Reactions involving pyrite are either endothermic or exothermic, depending on whether oxidation is involved. Oxidation reactions can contribute 107-320 MJ/t per wt% S in raw shale (14).

Not all of the reactions in Table 1 will occur in a specific shale retorting system. One reason is that shale can lack the required mineral constituents. For example, the saline minerals nahcolite (2NaHCO₃) and dawsonite (2NaAl(OH)₂CO₃) are present in large quantities in the saline zone of the GRF, but will not be present in large quantities in most shales undergoing retorting (<1 wt% in the Mahogany zone). Another reason is that some retorting processes will discourage reactions. For example, during in situ retorting (like the Shell in situ conversion process - ICP), the dolomite and calcite reactions will not occur to any significant extent because of the low retorting temperature.

A complication that prevents generalizations about heat demand from mineral reactions is that endothermic decomposition of a species can result in differing thermal demand depending on the end products generated. For example, the reaction of CaCO₃ with SiO₂ (reaction 2 in Table 1) has about half the thermal demand of decomposition of CaCO₃ to CaO and CO₂ (reaction 1). The relative strength of these reactions is governed by the partial pressure of CO₂ during retorting, which varies with the process used (16).

As a simple example, a GRF oil shale that is (by weight) 25% ankeritic dolomite, 12% calcite, and 1% nahcolite, retorted in a surface retort fueled by shale char combustion, could experience approximately 50% decomposition of

³ This is calculated using their enthalpy relationship $H(773\text{ K}) - H(298\text{ K}) = 569 + 1.181G$, where G is the FA yield in l/t. Similar relationships were found in two earlier studies (15).

the dolomite, 10% decomposition of the calcite, and complete decomposition of nahcolite. If 80% of the calcite CO₂ is emitted through the silicate reaction,

Table 1: Enthalpy change with mineral reactions^a

<i>Reaction</i>	<i>T (°C)</i>	<i>ΔH (J/g or MJ/t)@ 298K</i>
Calcite:		
1. CaCO ₃ = CaO + CO ₂	600-900	1764
2. CaCO ₃ + SiO ₂ = CaSiO ₃ + CO ₂	700-900	878
3. 2CaCO ₃ + SiO ₂ = Ca ₂ SiO ₄ + 2CO ₂	700-900	1133
Dolomite:		
4. CaMg(CO ₃) ₂ = CaO + MgO + 2CO ₂	600-750	1680
5. CaMg(CO ₃) ₂ = CaCO ₃ + MgO + CO ₂	600-750	715
6. CaMg(CO ₃) ₂ + 2SiO ₂ = CaMgSi ₂ O ₆ + 2CO ₂	700-900	849
7. CaMg(CO ₃) ₂ + SiO ₂ = CaMgSiO ₄ + 2CO ₂	700-900	1049
Saline minerals:		
8. 2NaHCO ₃ = Na ₂ CO ₃ + CO ₂ + H ₂ O	100-150	1324
9. 2NaAl(OH) ₂ CO ₃ = Na ₂ CO ₃ + Al ₂ O ₃ + 2H ₂ O + CO ₂	350-400	842
10. NaCO ₃ + 2SiO ₂ = Na ₂ Si ₂ O ₅ + CO ₂	700-900	849
11. NaCO ₃ = Na ₂ O + CO ₂	>850	3031
Dehydration of clays ^{b,c}	Various	2555
Pyrite:		
12. FeS ₂ + 2H = FeS + H ₂ S (during pyrolysis)	440-475	523 ^d
13. FeS ₂ + H ₂ O + C = H ₂ S + FeS + CO (w/ steam)	350-500	1619
14. FeS + H ₂ O = FeO + H ₂ S (w/ steam present)	450-700	572
15. 2FeS ₂ + 5½O ₂ = Fe ₂ O ₃ + 4SO ₂	<600	-6900

a – Values are from Campbell (16) except that for clay (13) and sulfur reactions (17, 18). The experimentally derived Δ*H* for some of these reactions was observed to be somewhat smaller than values from the reference literature (16, Table 7).

b – The dehydration of clays must also include a correction term to the heat capacities of hydrated minerals to account for the heat capacity addition due to the bound water before it is liberated. Camp (13) cites a heat capacity value of 1.68+0.0022*T* (temperature in K) for bound water, which is lower than that for free water.

c – The clay dehydration data of Camp (13) includes all clays as a single species.

d – Depending on the source of the hydrogen donor, this reaction could be more or less endothermic.

(Reaction 2), then the total thermal demand from mineral decomposition will be ≈ 130 MJ/t of shale processed. Note that this is a significant fraction of the heat of retorting. In a low-temperature process (e.g., conductive in situ retorting), this thermal demand will be greatly reduced because carbonate decomposition will be limited.

Lastly, because of factor (d), the amount of water that must be driven off of the shale can contribute significantly to the heat of retorting. This water can be free water or water bound to clays or other mineral matter. Bound water has a lower heat capacity than free water because it has less vibrational freedom than liquid water (13). But the energy burden of dehydration is larger than the heat of vaporization. Replacing 1 wt% of mineral matter with free water will result in ≈ 20 MJ/t addition to the heat of retorting, while adding the same amount of bound water would add ≈ 30 MJ/t (13).⁴

All of the above factors make it difficult to generalize about the heat of retorting. There is a large diversity of oil shale processes and oil shale types. And even for what is nominally the same type of process, the details of the engineering implementation can affect the thermal history of the shale, which affects the heat of retorting. Consequently, each process must be analyzed in detail before reliable estimates can be made of the amount of CO₂ generated from retorting energy inputs.

Illustrative estimates of the general heat of retorting demands can, nevertheless, be made for three cases of GRF shale⁵ retorting:

- a) Slow in situ retorting (0.5°C/day) to 350°C,
- b) Fast retorting to 515°C at 30°C/min heating rate, and
- c) Fast retorting to 515°C as above with the spent shale used as at heat carrier and heated to 750°C. In this case there is heat recovery from the spent shale (as in the ATP retort).⁶

⁴ The exact difference will depend on the heat capacity of the mineral species contained in the shale. It will also change with the heats of dehydration for bound water, which are uncertain (13). Nevertheless, the heat capacity of water is ≈ 4 times that of shale mineral matter, and the heat of vaporization or dehydration is significant, resulting in an energy burden from additional water content (on a volumetric basis water has ≈ 2 times the heat capacity because it is less dense).

⁵ In the cases outlined, shale has the mineral composition from Camp (13), specifically: 16.7% organic matter (≈ 110 l/t), 25% ankeritic dolomite with the formula $Mg_{0.72}Fe_{0.28}(CaCO_3)_2$, 15% calcite, and 1.3% bound water.

⁶ This calculation uses a simple model to account for carbonate decomposition. It uses the Thorsness (19) OSP model (described below) and assumes a mass-

The resulting heats of retorting for these three cases are outlined in Table 2.

Table 2: Estimated heats of retorting for three illustrative cases^a

	<i>Unit</i>	<i>Case a</i>	<i>Case b</i>	<i>Case c</i>
Heating rate	K/sec	5.8x10 ⁻⁶	0.4	0.4
Final temperature	°C	350	515	515/750
Dolomite decomposition	%	0	< 2	45
Calcite decomposition	%	0	~ 0	2
Enthalpy of retorting	MJ/t raw shale	450	730	520-670^b

a – These heats of retorting calculated using the shale characteristics described in footnote 5.

b – This includes a total heat demand of 820 MJ/t, with heat recovery from spent shale of 150 – 300 MJ/t of raw shale. This value is only approximate because the amount of heat recovery depends on the specifics of operation of the retort.

Lastly, the efficiency of thermal energy transfer to shale also must be accounted for. Thermal losses to the surroundings through the retort shell (in ex situ retorting) or to the surrounding formation (during in situ retorting) will increase the thermal energy requirements of retorting. Data suggest that between 5% and 20% of the heat may be lost during retorting (6, 20).

The heat of retorting values calculated in MJ/t for a given retorting process, can be converted to CO₂ emissions using the CO₂ intensity of thermal energy sources (Table 3). Care is required when electricity is used as the thermal energy source because the carbon intensity of electricity can vary significantly depending on its primary energy source, the efficiency of generation, and transmission losses. We see that for natural gas used directly in case *a* (as with natural-gas-fired downhole heaters), emissions might be 22.5 kgCO₂/t shale processed, while the use of char in case *b* might result in emissions of nearly 70 kgCO₂/t shale processed, if char combustion could be accomplished without carbonate decomposition. The use of electricity will, in general, increase these values. These carbon intensities of the thermal demand of retorting can be converted to fuel basis, and they range generally between 10 and 20 gCO₂/MJ RFD.⁷

weighted residence time at 750 °C of 9.5 min. This results in significant decomposition of dolomite, but not significant decomposition of calcite.

⁷ We assume here: a 110 l/t shale is retorted, with 95% of FA liquid yield recovered; the shale oil has characteristics of Paraho raw shale oil (21) (HHV = 44.4 MJ/kg, API gravity = 21.4); there is 90.1% energetic conversion to refined products output (see discussion below); and 10% of thermal energy inputs to

Table 3: Carbon intensity of thermal energy sources

<i>Thermal energy source</i>	<i>Carbon intensity of thermal energy sources</i>		<i>Source</i>
	<i>Carbon density (gC/g fuel)</i>	<i>CO₂ intensity (gCO₂eq./MJ)</i>	
Natural gas	> 0.75	49-51	(22)
Coal	< 0.75 to > 0.92	88-97	(22)
Shale char ^a	0.87 to 0.92	88-100	(23)
Electricity - Nat. gas ^b	NA	111	
Electricity - Coal ^c	NA	280	
Electricity - Colorado ^d	NA	206	(24)

a – These values from formulas for char produced from secondary pyrolysis at $\approx 550^{\circ}\text{C}$ and tertiary pyrolysis at $\approx 750^{\circ}\text{C}$ (23, *Table 3*). HHV of the char is calculated using the Dulong formula. This does not include the associated carbonate decomposition.

b – Assumes combined-cycle turbine with 45% efficiency of generation and transmission. Assumes 50 gCO₂/MJ natural gas.

c – Assumes pulverized coal boiler with 30% efficiency of generation and transmission. Assumes 92.5 gCO₂/MJ of coal.

d – Data from EIA (24) for total electricity generation (MWh) and total emissions (Mt CO₂) in Colorado.

Carbon dioxide emitted due to auxiliary energy use in the retorting process

Carbon dioxide is also emitted due to energy consumed in non-thermal energy requirements of retorting. For ex situ retorts, these non-thermal energy uses include: mining the raw shale, transport of raw shale to the retort, crushing and pre-processing raw shale, operation of the retort, transport of spent shale to disposal site, and handling of crude shale oil. For in situ retorts, the mining energy requirements above are replaced with drilling and casing wells, along with other subsurface operations. These miscellaneous emissions are difficult to calculate without actual project data, as they depend on specifics of a given facility.

In one report of emissions from the ATP ex situ retort, emissions from electricity consumption and mining diesel use were estimated at 11.3 and 10.3 gCO₂/MJ RFD, respectively (25, *p. 104*). In a report of emissions from ATP

retorting are wasted by loss to the surroundings. These values result in crude shale oil yield of 4300 MJ/t, and refined fuel yield of 3875 MJ RFD/t.

technology applied to the Stuart shales of Queensland, emissions from electricity and diesel use were reported to be 8.0 and 0.3 gCO₂/MJ RFD, respectively (26).

For an in situ case, an analysis of the Shell ICP suggests that emissions from non-thermal retorting energy use were between ≈ 4 and 8 gCO₂/MJ RFD, for uses such as drilling, freeze wall maintenance, pumping, and site reclamation (6). These are estimates not based on data from commercial scale operations, and were conservatively calculated, so actual emissions could be higher.

Carbon dioxide emitted from oil shale

Lastly, CO₂ is emitted from shale during retorting. This is due to two processes that occur with the heating of shale: formation of CO₂ from kerogen and bitumen, and formation of inorganic CO₂ from mineral reactions.

Organic CO₂ is emitted in retorting due to the elimination of existing oxygen in the organic matter as CO₂ in the presence of retorting heat. Because the chief reaction is thought to be decarboxylation of organic acids and esters within the kerogen, the amount of CO₂ generated in this manner scales with the organic content of the shale and has little to do with the mineral content of the shale (23).

Kerogen from Green River oil shale contains 5 to 6 wt% oxygen (see Table 4), while raw shale oil contains only trace amounts of oxygen. In theory this means that up to 8% of the mass of kerogen contained in the shale could leave as CO₂ if all organic oxygen were converted to CO₂. In practice, however, water vapor is also formed. Empirical results from Stanfield (27) reported that 2.4% to 4.7% kerogen mass is emitted as CO₂,⁸ whereas more recent analyses suggest values ranging from 4.1% to 5.3% of kerogen mass (23, 28).⁹ A study of 66 shale samples (30) provides a well-grounded correlation for CO₂ yield, including both mineral and organic CO₂, as a function of shale grade (see Figure 1). From this and other data, 4.1% of the kerogen mass is emitted as CO₂.¹⁰ Thus, for shale that is 16% organic matter, emissions will be 6.5-8.5 kgCO₂/t shale processed, or 1.7-2.2 gCO₂/MJ RFD.

Organic CO₂ is emitted before the peak rate of oil generation, with peak generation occurring at around 400°C in the FA (23, Figure 3). Later reactions

⁸ These values are for 4 samples of GRF oil shale ranging from 44 to 257 l/t richness.

⁹ The Huss and Burnham data also include CO, which oxidizes quickly in the atmosphere and is therefore included in CO₂ emissions estimates (29, p. 2-8)

¹⁰ This value also includes carbon in CO, as it is quickly oxidized to CO₂ in the atmosphere. This value is lower than some other studies, possibly because the fraction of oxygen in kerogen was overestimated in prior studies due to oxidation during analysis.

such as secondary and tertiary pyrolysis (>550°C and >750°C, respectively) do not result in organic CO₂ emissions because the oxygen has been consumed well before these temperatures are achieved (23).

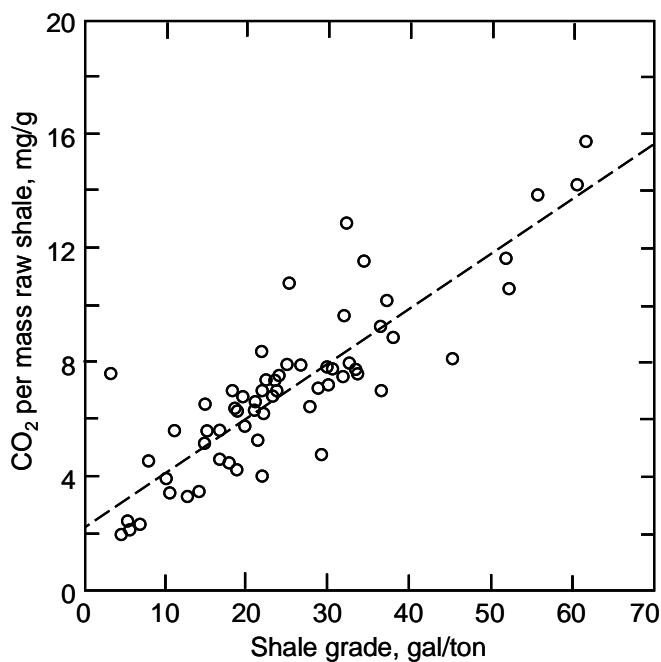


Figure 1: CO₂ yield as a function of shale grade for 66 Green River oil shale samples [adapted from (30)]. The non-zero intercept probably represents CO₂ from nahcolite at an apparent concentration of 0.8 wt%.

If a retorting process occurs with oxygen input, as in a directly heated ex situ retort, the emissions of CO₂ from organic sources will be a combination of CO₂ derived as above, and CO₂ derived from the combustion of organic material to provide retorting process heat. These emissions were covered above in the thermal requirements of retorting.

Additional CO₂ is emitted from shale due to reactions of inorganic mineral matter during retorting. The most important of these reactions were listed and numbered in Table 1.

Table 4: Composition of kerogen in Green River shale

	<i>Elemental kerogen composition (wt %)</i>			
	<i>Smith^a</i>	<i>Singleton et al.^b</i>	<i>Campbell et al.^c</i>	<i>Huss and Burnham^d</i>
Carbon	80.52	80.97	80.32	81.72
Hydrogen	10.30	10.19	10.31	10.22
Nitrogen	2.39	2.36	2.62	3.05
Sulfur	1.04	1.08	1.07	-
Oxygen	5.75	5.36	5.68	5.01

a – These values are the average of 10 sample of cores of Mahogany zone oil shale from Colorado and Utah. The composition across samples was reported to be very consistent. Source: (11, Table 33).

b – Source: (30), based on the empirical formula derived from 66 Green River shale samples: $\text{CH}_{1.50}\text{N}_{0.025}\text{O}_{0.05}\text{S}_{0.005}$.

c – Source: (28) This is based on the empirical formula $\text{CH}_{1.54}\text{N}_{0.028}\text{S}_{0.005}\text{O}_{0.053}$, derived from shale from the Anvil Points Mine.

d – Source: (23) This is based on the empirical formula $\text{CH}_{1.50}\text{N}_{0.032}\text{O}_{0.046}$, derived from 7 samples of varying organic content from the Anvil Points Mine and Colorado lease tract C-a.

Common saline mineral reactions (such as decomposition of nahcolite and dawsonite, reactions 8 and 9 in Table 1, respectively) occur at low temperatures. Because these temperatures are below those at which retorting occurs, these minerals will completely decompose during retorting. Thankfully, these minerals are not prevalent except in the saline zone of the GRF. For every 1 wt% of nahcolite that decomposes, 2.6 kgCO₂/t is emitted. The decomposition of carbonate minerals dolomite and calcite occurs at higher temperatures and will therefore be most problematic in retorting systems where the spent shale is combusted to utilize the heating value of the shale char. For every 1 wt% of dolomite that undergoes primary decomposition (reaction 5), 2.3 kgCO₂/t is emitted, whereas the same figure for calcite (reaction 1) is 4.4 kgCO₂/t.

There is uncertainty about the kinetics of carbonate decomposition in shales. This is partly due to the difficulty of modeling the complex reactions in a heterogeneous substance such as oil shale (16). Some generalities about the mineral reactions do, however, exist. First, decomposition increases with both the maximum temperature achieved and the amount of time spent at that temperature (Figure 2). Also, the primary decomposition of dolomite (reaction 5) occurs much more quickly at low temperatures than calcite decomposition.

Also of great importance is that simple decomposition of calcite (reaction 1) is significantly inhibited by the presence of gaseous CO₂. This can be seen in the divergence in Figure 2 between the decomposition of calcite at 0.25 atm CO₂ (dashed lines) and 1 atm CO₂ (solid). The temperature at which decomposition begins increases with higher partial pressures of CO₂, and the dominant reaction changes from reaction 1 to reactions 2 and 3 (Table 1). Given the likely high partial pressures of CO₂ in the immediate gaseous environment of retorting particles, most CO₂ release from calcite will occur from the reaction of calcite with silica, rather than decomposition to CaO.¹¹

Despite these regularities, there are significant differences in the reaction rates found by different models of carbonate decomposition. Campbell (16) reported reaction kinetics for carbonate decomposition processes in shale. More recently, Thorsness (19) reported two models: the OSP model, which was based on the work of Jukkola (31), and a “Fast Kinetics” model based on results from the Lawrence Livermore National Laboratory (LLNL) 4TU-Pilot retort.

The OSP model is in general agreement with Campbell’s decomposition model (results from this model are presented in Figure 2). Unfortunately, this model performed poorly in predicting decomposition in the LLNL retort, with predictions 12-17% low on an absolute basis (a significant deviation when absolute decomposition rates tend to be below 50%). Thorsness created the Fast Kinetics model to match empirical data from the LLNL retort. This model predicts very high levels of carbonate decomposition, significantly in excess of those predicted by Campbell and the OSP model. Also, this model was not generated for modeling in situ retorting, so the usefulness of this model under those conditions is unknown (e.g., it is thought to overestimate rates of decomposition at slow heating and low temperatures).

As an example of the divergence between model results, the OSP model predicts decomposition of dolomite of 24% and 50% when shale is heated to 700°C for 2 minutes and 5 minutes, respectively. On the other hand, the Fast Kinetics model predicts decomposition fractions of 79% and 98% for the same conditions. This gross divergence suggests that more research on carbonate decomposition is needed. Part of the solution may be the use of fractional order kinetics, as would be expected for shrinking core reactions.

¹¹ In Campbell’s (16) empirical results, simple decomposition of CaCO₃ was only dominant at P_{co2} = 0, a condition not likely to hold for any period of time in the atmosphere directly surrounding decomposing shale mineral matter. At higher partial pressures of CO₂, the overwhelming reaction was with silica (16, Table 4). Overall, the silica reaction resulted in about 4/5 of the evolved CO₂ (16, Table 7).

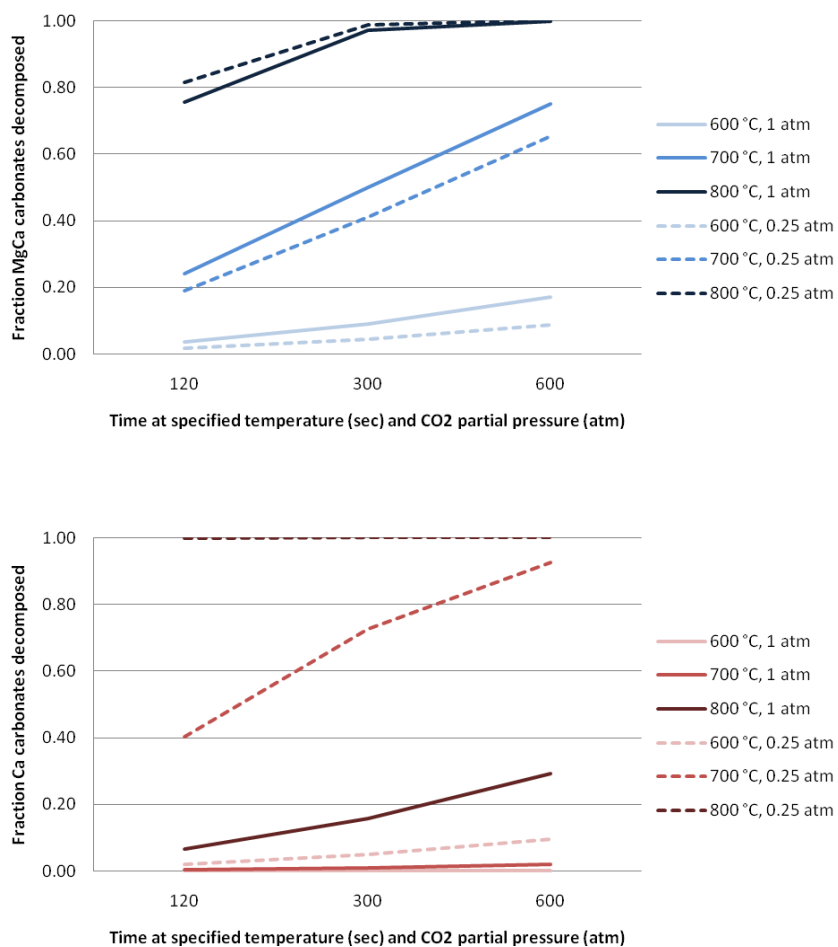


Figure 2: Fraction of carbonate minerals (calcite bottom, dolomite top) decomposed as a function of time (x-axis) and temperature (y-axis). Kinetics based on OSP model (19). In dashed lines the partial pressure of CO₂ is assumed to be 0.25 atm, whereas for solid lines it equals 1 atm. Note the very strong response of calcite to CO₂ pressure.

Upgrading and refining of oil-shale-derived hydrocarbons

After crude shale oil is produced, it must be upgraded and refined. This upgrading can include anything from simple stabilization of the raw shale oil for transport to complex fractionation and upgrading systems (32). At least some upgrading is required before refining, because raw shale oil, at least from the GRF, is generally:

- a) Unstable and therefore not able to be pipelined due to formation of gums (33);
- b) Affected by suspended solids which must be removed;¹²
- c) High in nitrogen content (approximately 2%, compared to about 0.2% for conventional crude oils); and
- d) High in arsenic, iron and nickel (21, p. 1005).

It is difficult to generalize about oil shale upgrading (21). This is because the properties of raw shale oil differ greatly depending on the retorting process used and the raw shale retorted. For example, the Paraho retort produces 21°API crude, while tests of the Shell ICP process have produced crudes of 36°API (34) with substantially lower nitrogen and metals content. The energy inputs to and emissions from upgrading will also vary because numerous upgrading pathways and technologies are possible (21).

Due to this variability, wide ranges of hydrogen requirements for upgrading are cited. Speight cites H₂ requirements of between 1400 – 2060 scf H₂/bbl of raw shale feed (21). Probstein and Hicks reported that upgrading of Paraho crude would have a stoichiometric hydrogen demand of 2.1 kg H₂ per 100 kg of raw shale oil (32).¹³ They reported that actual demand could be nearly twice this high, or 40 m³ H₂/100 kg shale oil, due to the formation of H-rich HC gases. More recently, Johnson *et al.* reported energy requirements of 126.6 MJ/bbl of raw shale feed (35).

These values are converted to consistent units of gCO₂/MJ of crude shale oil feedstock below in Table 5.¹⁴ This table shows that there is considerable variation in the figures, especially considering the much lower value implied by the energy use cited by Johnson *et al.*

¹² For example, shale oil produced by the Paraho retort contained 0.5 wt% suspended solids, most of which settled out after the oil/water emulsion was broken. About 250 ppm of fine solids remained after settling (21, p. 1011)

¹³ This calculation assumed upgrading from CH_{1.59}O_{0.014}N_{0.02}S_{0.003} to finished crude of CH_{1.8} plus water, ammonia, and H₂S.

¹⁴ In this table, we assume as in Probstein and Hicks (32) that the total energy use in upgrading is approximated by the hydrogen demand.

Table 5: Estimates of hydrogen requirements of shale oil upgrading, converted to emissions of CO₂.

	<i>Case</i>	<i>Reported requirements</i>		<i>Emissions</i>
		<i>Value</i>	<i>Unit</i>	<i>gCO₂/MJ crude shale oil</i>
Speight (21)	Low	1400	scf H ₂ /bbl	4.93 ^a
	High	2060	scf H ₂ /bbl	7.25 ^b
Probstein and Hicks (32)	Low	2.1	kg H ₂ /100 kg shale oil	4.30 ^c
	High	40	m ³ H ₂ /100 kg shale oil	7.31 ^d
Johnson <i>et al.</i> (35)	-	126.6	MJ/bbl of shale oil	0.97 ^e

a – Value from Speight (21, p. 1028) for hydrocracking of oil from Occidental MIS retort. Converted to CO₂ emissions using efficiency and CO₂ emissions from modern steam methane reformation, which equal 9.1 gCO₂/g H₂ produced, assuming efficiency (LHV basis) of 76% (36).

b – Value for hydrocracking of Paraho crude. CO₂ emissions calculated as in note a.

c – Minimum stoichiometric demand for hydrotreatment of Paraho crude. See text for explanation. CO₂ emissions calculated as in note a.

d – High estimate of actual demand for hydrotreatment of raw shale oil. CO₂ emissions calculated as in note a.

e – For upgrading 21 °API raw shale oil to 38 °API. CO₂ emissions calculated assuming natural gas is feedstock energy source for upgrading.

After upgrading of the crude shale oil, it must be refined into finished liquid fuels.¹⁵ In 2006, U.S. refineries had the following gross characteristics: 39.1 EJ of crude oil and other feedstocks were taken in; 2.2 EJ of feedstock inputs were consumed for energy needs during refining; and 1.8 EJ of purchased outside energy was also consumed. Total energetic output in products was 35.2 EJ, whereas refined fuel products output (less asphalt and “miscellaneous” output) was 33.8 EJ (37).

Thus, in the aggregate, for every 1 MJ of crude oil input, 0.901 MJ of products were produced, and 0.864 MJ of refined fuels were produced. The resulting combustion CO₂ emissions amount to 7.7 gCO₂/MJ of total product

¹⁵ In all calculations present here, we assume for simplicity that upgraded synthetic crude has the same energy content as the raw crude oil input to the upgrading process (32, see p. 357)

output, or 8.0 g CO₂/MJ refined fuels.¹⁶ The energy and carbon intensity of a specific refined fuel will differ from this average value. For example, reformulated gasoline has 1.15 to 1.3 times the energy intensity of the average refinery output (38), and will therefore have higher emissions. For example, in the GREET model, a full fuel cycle emissions model from Argonne National Laboratory, total emissions from reformulated gasoline production are 12.4 gCO₂/MJ RFD, significantly higher than the average values calculated above.

The energy intensity and CO₂ emissions from refining upgraded shale oil will differ depending on the degree of upgrading. Minimal upgrading would likely result in refining emissions that are higher than these aggregate values for U.S. refineries, due to the lower quality of partially-upgraded shale oil. However, more extensive upgrading would result in lower refining emissions than for conventional crudes. This is because the degree of upgrading required to remove the nitrogen and arsenic compounds present in raw shale oil will also result in near-elimination of sulfur and a reduction in the undesirable high-molecular-weight fraction of the shale oil (21).¹⁷ This will lead to a higher proportion of liquid fuel product outputs from a given input of upgraded shale oil.

Given the uncertainties involved, we make simple and conservative assumptions for this chapter:

- a) That preliminary upgrading is moderate to high in intensity, and results in emissions of 5 gCO₂/MJ of refined fuel delivered;
- b) That the upgraded product delivered to refineries is of high quality so that the emissions from reformulated gasoline production equal to ¾ of those from conventional feedstocks. This gives a result for emissions from refining of 9.3 gCO₂/MJ of refined fuel delivered.

Using these assumptions, total upgrading and refining emissions for production of reformulated gasoline from shale oil amount to 14.3 gCO₂/MJ RFD, whereas those for conventional petroleum from the GREET model total 12.4 gCO₂/MJ RFD.

¹⁶ This emissions estimate is calculated by applying fuel-specific emissions factors to all of the fuels consumed in refining, both those produced internally (such as coke and still gas and residual oils) and those purchased from external energy suppliers (such as purchased electricity, natural gas, or steam). In addition to these combustion emissions, non-combustion emissions from refining also exist.

¹⁷ For example, Paraho crude upgraded by Sohio or LETC hydroprocessing had very low sulfur concentrations (0.02 - 0.05 wt%), and LETC hydroprocessing reduced the residuum fraction of shale oil (> 1000°F) from 12.7 wt% of the raw crude to 2.7 wt% of the upgraded crude.

Carbon dioxide from combustion of shale-derived gasoline and diesel

Carbon dioxide emissions from the combustion of shale-derived liquid fuels will be generally equal to those from fuels derived from conventional petroleum. This is because shale-derived fuels will be refined to the same standards as conventionally-derived fuels. The carbon intensity of the refined fuel assumed here (U.S. Federal standard reformulated gasoline) is 67.2 gCO₂/MJ (22).

Carbon dioxide from materials inputs to extraction

In addition to direct emissions from the three stages of the fuel cycle, comprehensive CO₂ accounting necessitates counting indirect or “embodied” emissions from the manufacture of capital and material inputs to oil shale extraction technologies (39).

For example, for the Shell ICP (6), indirect emissions were calculated for the following inputs: steel used in well casing, surface collection equipment, and facilities; cement used in well casing and facilities; and HDPE piping. Total embodied energy was calculated at 30-35 MJ/t shale processed, the majority of which is consumed for steel manufacture. This energy demand results in emissions of < 1gCO₂ eq/MJ of refined fuel delivered.¹⁸

Except in the most capital intensive of operations, indirect emissions will tend to be very small when compared to direct emissions. This is true for both shale-derived fuels and conventional petroleum-based fuels. In fact, such values will generally be within the uncertainty range of emissions from any given shale retorting process.

Uncertainty in magnitude of carbon emissions

The discussion above illustrates that there is significant uncertainty with regard to emissions from oil shale production depending on what process is used. This uncertainty is primarily present in the retorting process stage; emissions from refining and combustion of refined fuels are more easily defined. One aspect of these uncertainties is explored further below in an industry-scale model of one particular implementation of in situ shale oil production that uses electric power as a heat source. This model explicitly includes distributions of shale properties (such as shale richness), and uses these distributions to calculate probabilistic emissions from an industry producing 3 Mbb/d of crude shale oil.

¹⁸ Often, embodied emissions are difficult to calculate because it is unclear which fuel is used in each manufacturing process. Here we assume the carbon intensity of consumed fuels is on average equal to diesel fuel.

Probabilistic Model for CO₂ Generation from Production of Shale Oil

Boak (4) presented a simplified model developed for the output of CO₂ from retorting processes. Three sources of CO₂ are included – power plant emissions, mineral reactions, and kerogen – using data on the processes available in the public domain. The model runs in Lumina Decision Systems' *Analytica*TM, a visual tool for creating, analyzing, and communicating decision models. *Analytica*TM performs multiple calculations using a Monte Carlo algorithm to provide a statistically-based distribution of results for calculations involving uncertain parameters, and is especially useful for probabilistic modeling where many variables are uncertain. It is relatively easy to evaluate the importance of uncertainties in the model result, and therefore determine what parts of the model most require refinement. In addition, the system supports linking of variables in a graphical manner, making the model relatively transparent, so that anyone can reasonably understand how the model calculates a result.

Currently, the model only includes emissions from the retorting portion of the fuel cycle (that is, it does not address CO₂ emissions from upgrading and refining, or CO₂ released by burning the resulting fuel). This approach captures most of the uncertainty with a relatively simple model. The model calculates the impacts of a large oil shale industry with 3 mbbbl/d output of crude shale oil.

The model is expected to capture the range of possible values, and to provide insights into the problems that may need to be addressed to define better the likely emissions of an oil shale industry. The model was refined for calculations supporting this chapter and a more detailed description of the model is underway.

Modeling methods

The estimated release of CO₂ from natural gas fired power plants is based upon a value of 50.2 gCO₂/MJ (40), with an estimated uncertainty applied based on Boak (4). This value is in accord with the number for natural gas in Table 3, before adjustments to reflect the efficiency of the power plant. The calculations for this chapter assume an efficiency range from 40-55%, which allows for some understanding of the effect of power plant efficiency, including the potential for improvements in natural gas power plant efficiency. The quantity of electricity is very large, so electricity supply might be diversified, at least until production reaches levels justifying dedicated power plants. It would be valuable to develop a specific scenario that included both the energy efficiency and carbon output presuming some fraction of power comes from lower efficiency coal-fired power plants. No allocation was made of additional energy expended in

maintaining the freeze wall to contain the local ground water. In this respect the model is non-conservative. However, the model also did not consider the potential to preheat a block of rock using heat recovered from a previously heated block.

Boak (4) used the estimate of Burnham and McConaghy (41) for the amount of energy required to retort oil shale of (87-124 kWh/t) in the range from 300-400°C. This range is somewhat lower than in Table 2, in part, because it does not include energy to dry the shale. The values shown in this chapter were calculated from a baseline value for the mineral content (323.5 MJ/t) and adjusted for water content (27 MJ/t per weight percent water) and kerogen content (4.345MJ/t for each FA yield increase of 1 gallon/ton). Release of CO₂ from mineral reactions in the oil shale was estimated by presuming that any trace of nahcolite present in the rock would break down at temperatures below about 150°C (42) in accordance with reaction 8 from Table 1. Results from LLNL (30, 43) provide data on the amount of nahcolite present in the Mahogany zone of the Green River Formation. The average value is 0.8 wt %, in agreement with Figure 1. The range of values sampled is fairly large, so that the calculation may be somewhat representative of quantities of CO₂ released near heaters, where other carbonates may break down.

Additional CO₂ is released from the kerogen. Kerogen from the Mahogany zone of the Green River formation is estimated to contain 5.75 wt % oxygen on average, whereas shale oil contains 1.2 to 1.8 wt % (44). At the point at which the model was run, no information was available on the fraction of oxygen that might form CO₂ during in situ pyrolysis. So a mean value of 50% with a standard deviation of 15% was assigned. The value cited above of 4.1% of kerogen as CO₂ represents about 51% of the oxygen content of GRF kerogen.

Values for the amount of oil and gas produced were derived from results for Shell's in situ experiments, reported by Vinegar (45). Boak (4) assumed that an average of 78% of FA was removed from the rock as oil, and that gas was removed at an energy equivalent 30% of Fischer Assay oil. The average FA value for the entire industrial production was derived from average Fischer Assay values over the entire Green River Formation from 200 wells assembled by Y. Bartov at the Colorado School of Mines. All Fischer Assay data are tabulated by the U. S. Geological Survey. The Fischer Assay data were related to kerogen content based upon the relationship shown in Baughman (44), Figure 10. For the calculations shown here, the oil recovery was reduced, based upon personal communication with Shell personnel suggesting that, due to outward migration of a portion of the liquids, recovery is reduced to about 55-60% of FA yield.¹⁹

¹⁹ These yields are likely lower than commercial yields due to the high surface-area-to-volume ratio in the small ICP tests.

The model calculates oil and gas production from organic matter content and expected process efficiency. It calculates CO₂ both as tons/year and as SCF/day, which allows comparison to global CO₂ figures, but also allows comparison of the size of gas operations for production and separation.

Results

Results of the model are shown in Figures 3 through 8. The quantity of CO₂ generated annually varies by a factor of about eight from about 118 Mt (130 M ton) to one simulation (of 1000 runs) above 363 Mt (400 M ton). See Figure 3, which shows this distribution (probability units are fraction of runs that achieve the plotted value). The modal, median and mean are all in the vicinity of 190 Mt (210 M tons). The cumulative distribution of values is shown in Figure 4, which indicates that the probability of exceeding 225 Mt is less than 10%.

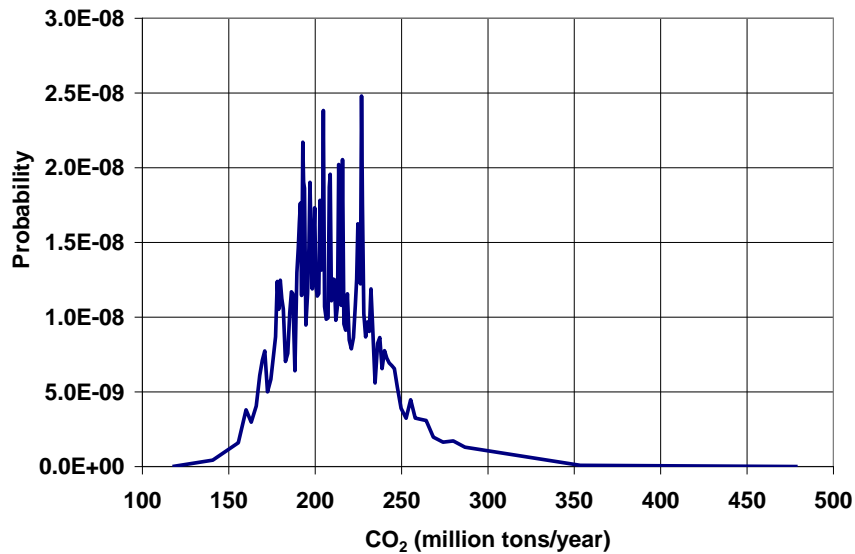


Figure 3: Annual CO₂ generation from oil shale production. To convert to Mt, multiply by 0.907.

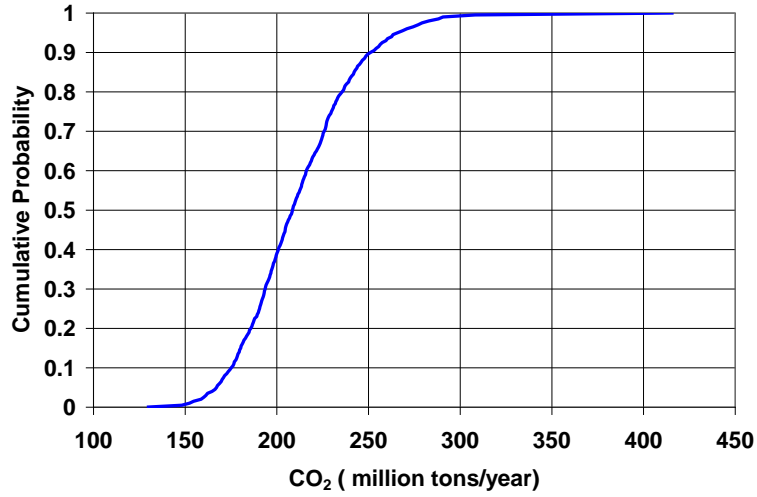


Figure 4: Cumulative probability plot for CO₂ release. To convert to Mt, multiply by 0.907.

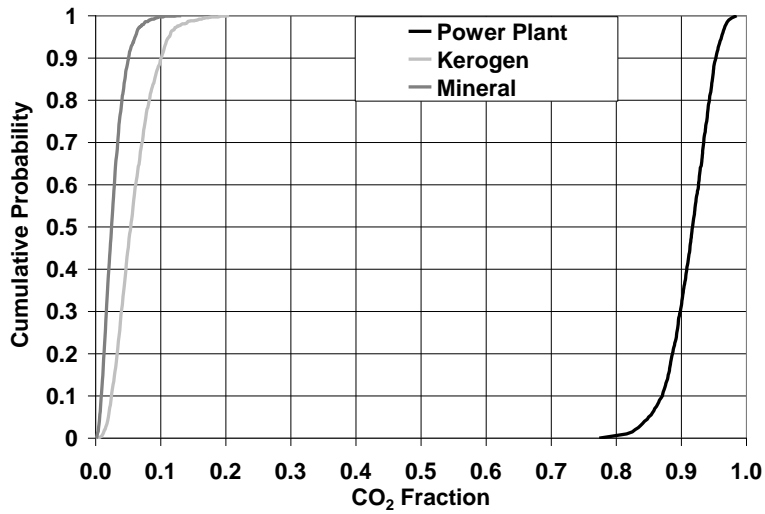


Figure 5: Fraction of CO₂ produced by the power plant, nahcolite mineral breakdown, and kerogen pyrolysis

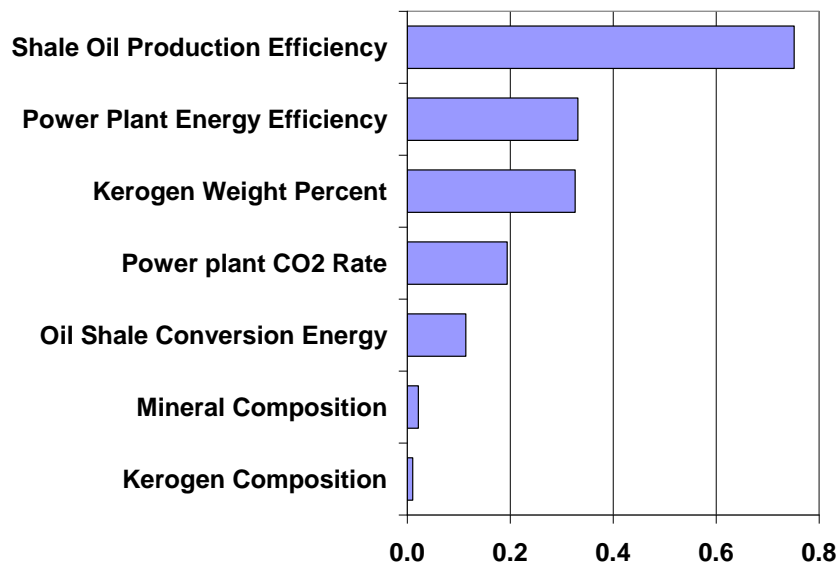


Figure 6: Importance of variables to CO₂ produced by oil shale

Figure 5 shows the fraction of the CO₂ produced by the power plant, which is greater than 90% at the midpoint of the range. The values for CO₂ generated from breakdown of trace nahcolite and kerogen pyrolysis may include values that are higher than is likely for an entire operating industry. As a consequence, revision of the model to more accurately reflect these fractions may well shift the distribution toward higher fractions coming from the power plant. This change could reduce the total quantity of CO₂ produced by in situ conversion.

Figure 6 shows the result of a sensitivity analysis of the outcome for total CO₂ production. It illustrates the importance of the various input parameters to the uncertainty in the output. The most significant variable is the Shale Oil Production Efficiency, the fraction of the Fischer Assay value recovered by the process. Experimental refinement of this value will be essential to better understanding of the CO₂ emissions.

Figure 7 shows the relationship between Fischer Assay (which is linearly related to the kerogen content, but provides a more familiar measure of oil shale richness). It indicates that, although the emission rates are around 350 Mt for one or two simulations, the bulk of the values lie between 135 and 250 Mt per year. The mean value of FA in the sampling distribution is ~100 l/t (~24 gallons/ton), which better represents the grade of oil shale that the industry will produce from in the GRF for many years. The efficiency of the power plant generating the

electricity for the downhole heaters is also important to the uncertainty of the emission estimate.

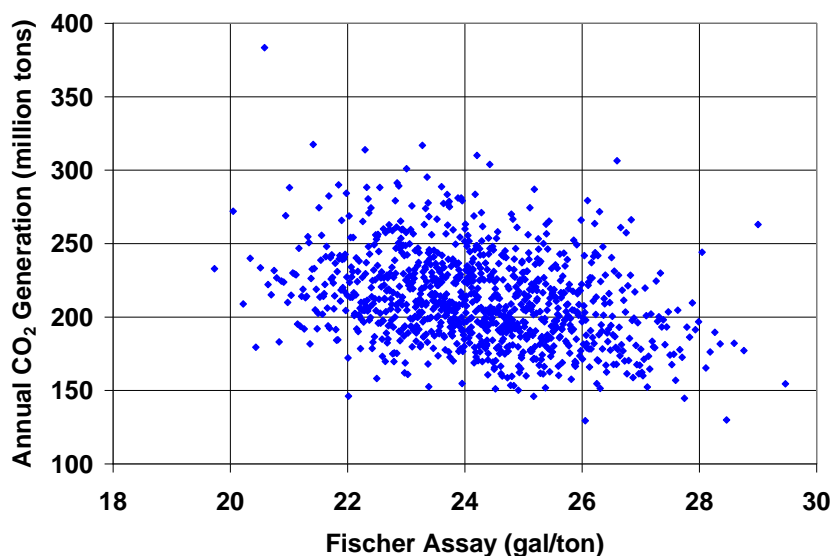


Figure 7: CO₂ produced as a function of average Fischer Assay of oil shale. To convert to Mt, multiply by 0.907.

Nahcolite decomposition and kerogen pyrolysis, although a minor fraction of the total CO₂ produced, can affect the quality of the gas produced. Figure 8 shows the relationship of CO₂ fraction in produced gas to the quantity of nahcolite and to the fraction of the kerogen oxygen that combines with carbon to make CO₂. The figure also shows the mean value assumed for each of the underlying parameters. Very few simulation results that have gas fractions of CO₂ greater than 0.10 result from below average fractions of one or the other (or both) of these two parameters. Even for values below one weight percent nahcolite, the fraction of CO₂ can be remarkably high. One other parameter, the kerogen content, is important to this result. Higher kerogen content provides a larger oxygen content to be converted.

The low temperature breakdown of nahcolite could result in an early pulse of CO₂-rich gas, which is unlikely to be a significant problem, as heating of the rock is uneven, which would provide mixing of this pulse. Higher temperature reactions (such as decomposition of dolomite) could be a problem at remarkably low levels of reaction. This is because they form a much larger fraction of the mineral matter. These reactions may occur during in situ retorting, but only in

the local environment near heater wells where temperatures could reach high levels. The production of other gases from mineral or organic matter is a possibility, which could dilute the CO₂ concentration in retort gas, which will affect the costs and prospects of capturing this CO₂ source for sequestration.

Uncertainty modeling conclusions

The quantities of CO₂ expected to be emitted by an oil shale industry are very large. A value of 190 Mt of CO₂ for an output of 3 Mbbbl/d is equivalent to 0.17 tCO₂ per barrel of crude shale oil produced, or 1.09 gCO₂/l. Assuming that the oil from this industry has the energy density of the 36 °API raw crude oil produced in Shell’s in situ retorting tests, this equals 28.6 gCO₂/MJ of raw shale oil. Low and high bounding estimates derived from the cumulative probability distribution in Figure 4 (10% and 90% probabilities) result in emissions of 24.7 – 34.1 gCO₂/MJ of raw shale oil produced.

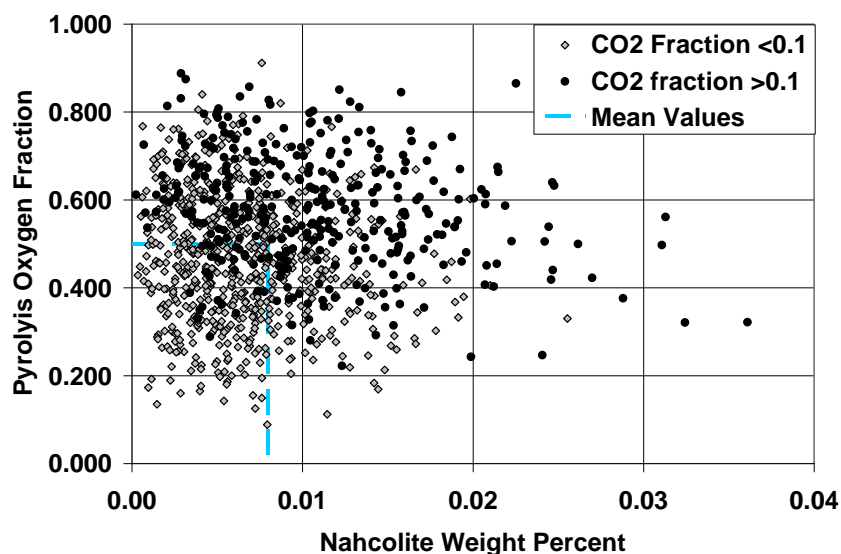


Figure 8: The fraction of oxygen removed from kerogen as CO₂ plotted against nahcolite weight fraction. Individual points reflect sampling of the range of uncertain parameters, and the symbols distinguish samples for which the resulting CO₂ fraction in the gas is less than or greater than 0.15.

Comparison of full-fuel-cycle carbon dioxide emissions estimates

Estimates of CO₂ emissions from oil shale retorting processes have been presented in the literature and in reports produced by oil shale producers. Here we convert these estimates to common terms and compare them to estimates of CO₂ emissions from conventional petroleum production and bitumen extraction and upgrading from the Athabasca tar sands.

In order to compare the estimates accurately, each was adjusted to consistent system boundaries and output products. For all cycles, we assume the end product is reformulated gasoline (U.S. Federal standard), upgraded and refined as described above. For each estimate, if a given process stage is not included, we use the default values for conventional petroleum refined to reformulated gasoline from the GREET fuel cycle model (46). For example, most of these estimates do not include transport of the reformulated gasoline from the refinery to the end consumer, so we add the default value of 0.45 gCO₂eq/MJ from the GREET model.

For ex situ retorting processes, we include two estimates of emissions from shales retorted in the Alberta Taciuk Processor (ATP), as compiled for environmental impact assessments by the project operators Southern Pacific Petroleum (SPP) and Oil Shale Exploration Company (OSEC) (25, 26). For comparison to the ATP results, we provide an estimate from the literature for a generic hot recycled solids (HRS) retort, of which the ATP is a specific type (8). For in situ retorting, we include two estimates of emissions from a low temperature in situ retorting process (Shell's ICP technology) (6), and one estimate of emissions from a modified in situ (MIS) retort (8). Lastly, we present a range of emissions generated from Boak's cumulative probability distribution (Figure 4), with the base case being the mean case discussed above (emissions equal to 190 Mt/y), and the error bars representing the 10% - 90% confidence interval. Because Boak focused on upstream emissions, we add upgrading, refining, transport and combustion emissions equal to the average of Brandt's low and high ICP cases. These estimates are plotted below in Figure 9. Note that the range of emissions presented is significant, from just over 100 gCO₂/MJ RFD to as high as 160 gCO₂/MJ RFD.

It is instructive to compare these emissions to other estimates from the literature:

1. estimates of emissions from tar sands mining, upgrading, and refining, which range from 96 to 101 gCO₂/MJ RFD (also for reformulated gasoline) (47).
2. estimates of emissions from tar sands in situ production (SAGD), upgrading and refining, which range from 100 to 111 gCO₂/MJ RFD for reformulated gasoline (47).

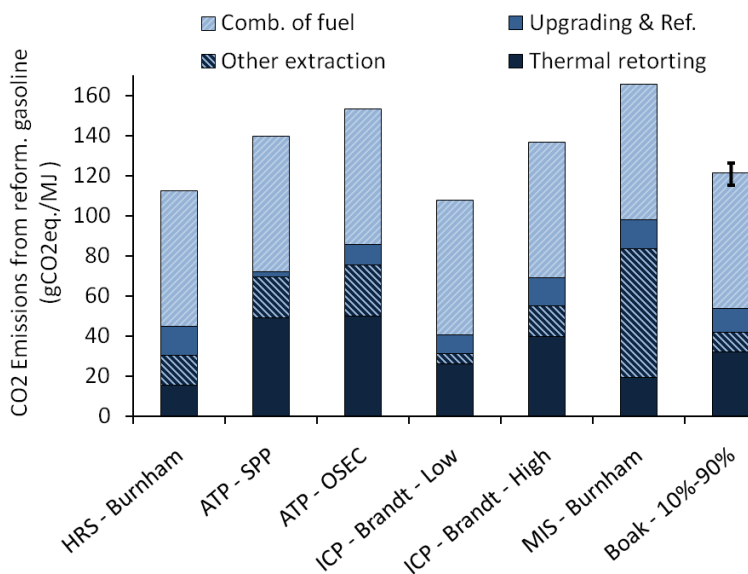


Figure 9: Estimates of CO₂ emissions from oil shale production processes. See text for sources.

- an estimate of emissions from conventional petroleum extraction and refining, which is 86 gCO₂/MJ RFD for reformulated gasoline production (46).

Given the uncertainties involved and the large range shown in Figure 9, a reasonable estimate of the emissions range is between 1.25 to 1.75 times those from conventional oil. These emissions are generally equal to or greater than those from oil sands production. In a future of low conventional oil availability, it is likely that the marginal hydrocarbon resource will be tar sands. If for this reason tar sands emissions are used as the basis for comparison, then oil shale will have a comparatively smaller emissions penalty. However, there is a strong desire to replace conventional petroleum with fuels that are less GHG intensive, thus we use conventional petroleum as the basis for comparison.

Of importance is that the highest emissions (from MIS retorting) are approximately 1.9 times the full-fuel cycle emissions from conventional reformulated gasoline production. But these high-carbon retorting systems (e.g., MIS retorting) are unlikely to be adopted: they would be very difficult to justify under carbon regulation, and at this time, this technology does not appear to be under consideration anywhere in the world. Importantly, there are a number of

ways of reducing this CO₂ emissions penalty by a factor of two or more by using a variety of methods described below.

Mitigation of carbon dioxide emissions

Boak's (4) industry-scale model described above (using gas-fired electric power) provides a central estimate of 190 Mt of CO₂ emitted per year from a 3 Mbbl/d in situ oil shale industry. United Nations data on CO₂ emissions by country for 2004 (48) show roughly comparable values: emissions from Saudi Arabia are approximately 300 Mt, and emissions from Thailand and Turkey are on order 200 Mt. Thus, a large oil shale industry in western Colorado would be a major global emitter. As another point of comparison, carbon dioxide emissions from flaring of stranded gas associated with oil production are reported to be approximately 400 million tons (49).

Given the potential scale of emissions, it is clear that mitigation of CO₂ emissions from oil shale development will be needed to comply with any future CO₂ regulation.

Methods of mitigating emissions

A variety of methods exist to mitigate CO₂ emissions from oil shale extraction. These include substitution of low-carbon primary energy sources, heat recovery and efficiency improvements, low temperature retorting to avoid carbonate mineral decomposition, and capturing and sequestering carbon emissions from retorts

The primary opportunity for reducing CO₂ emissions from oil shale retorting lies in the substitution of low- or zero-carbon energy sources for high carbon sources. Using the carbon intensities from Table 3, this clearly means avoiding the use of coal and shale char for process heat and encouraging usage of natural gas or co-produced HC gases. Substitution of natural gas for coal or char will nearly halve the carbon burden of retorting. For example, in Boak's industry-scale model described above, if all power were generated from the newest high efficiency gas turbines, it could reduce the emissions from the values presented here, perhaps by 10-15 percent. Even more radical reductions could be achieved through the use of near-zero GHG sources such as off-peak wind power (50), nuclear power (51) or solar power (52, 53) for retorting heat requirements. Replacing the retorting heat source with a near-zero-carbon energy source would bring emissions from oil shale-derived fuels quite near to those from

conventional oil production, as the CO₂ generation from mineral and kerogen reactions is less than 10% of the total.

These low-carbon energy resources tend to be more costly than the approximately free (shale char) or inexpensive (coal) high carbon energy carriers. This cost differential is the reason that less attention has focused on these energy sources in the past. But the future imposition of carbon regulation could significantly change the economics of fuel switching by rendering traditional high-carbon energy sources more expensive.

Another improvement might be made by switching from an electricity-based process to a thermal process. Depending on the depth of the resource and the need to protect aquifers, generation of thermal energy on the surface and sending it down into the formation, e.g., as proposed by EGL (54) and Petroprobe (55) could improve thermal efficiency. Even better, downhole generation of heat, as proposed by both Shell and EGL (56), could reduce the CO₂ emissions from retorting by about a factor of two from the gas-fired electricity case examined in the probabilistic model.

Improving heat recovery or reducing process heat losses will also result in lower emissions. These strategies are already practiced in existing retorting processes, due to the simple fact that they reduce operating costs. For example, in the ATP retort, countercurrent flow of hot spent shale preheats the incoming shale, driving off moisture and raising the shale to $\approx 250^{\circ}\text{C}$ before it enters the retort zone (57). In the case of in situ retorting, it might be economically feasible to recycle heat from a spent region to another region undergoing retorting. This could significantly reduce the energy requirements of retorting.

Efficiency improvements often involve reducing the heat losses through the boundary of the retorting zone. In the ATP retort, early patents noted that heat losses through the retort shell amounted to 20% of the thermal energy input (20, *column 19*), whereas in more modern incarnations of the ATP, heat losses through the shell have been reduced to 5-10% of the total demand (58). In the case of in situ retorting, increasing the size of the retorting region significantly reduces heat lost to over- and under-burden and the perimeter shale. Reducing these losses can significantly reduce the thermal demand and therefore the carbon emissions. The feasibility of this approach is limited by the economic risk involved with greatly increasing the scale of investment.²⁰ Other obvious efficiency improvements can result from reducing the waste associated with heat generation, as in switching from electricity to natural gas burned in down-hole burners for in situ processing. Such a change would eliminate the waste of \approx

²⁰ For example, an in situ operation spanning multiple km² would have negligible heat losses, saving large amounts of energy. However, the economic risk of such large investments would likely be prohibitive.

50% of the energy content of the natural gas, which occurs in even the most efficient power generation system.

Another method of reducing carbon emissions is to reduce the temperature achieved by shales that contain significant amounts of carbonate minerals. This can be done by retorting the shale slowly (e.g., in a conductive in situ retorting scheme) or by avoiding shale char as an energy source. Using shale char as the energy source involves combusting spent shale at temperatures where significant carbonate decomposition can occur (see Table 1). Even using spent shale simply as a heat carrier (e.g., heated with external combustion of natural gas) can result in the heating of carbonate minerals numerous times due to the recycling of spent shale through the retort zone.

Lastly, the CO₂ emissions from shale retorting could be captured and stored in geologic formations (36). This solution is generally capital and energy intensive, and will likely be considered after the other options addressed above. Capture is most effective and least costly when it is applied to a concentrated CO₂ stream. This reduces the cost of separating CO₂ from exhaust gases at diffuse concentrations (36).

A clear low-cost opportunity for capturing of concentrated CO₂ streams in oil shale retorting is from H₂ manufacture for upgrading. H₂ manufacture via steam methane reforming is readily adaptable to CO₂ capture, as the exhaust stream is already a CO₂-rich mixture (36). Concentrated CO₂ could also be captured at relatively low cost from pyrolysis gas, as the volume fraction of CO₂ can be quite high. A longer-term option for producing concentrated CO₂ streams is oxygen combustion, which removes the diluting N₂ before combustion rather than after combustion. The options for non-concentrated CO₂ capture include the emissions from power generation for oil shale retorting, such as from a natural gas combined cycle plant. This is a very large source, which will be critical to capture or eliminate. The more diffuse exhaust stream in power generation makes capture more difficult and costly. The cost of capturing CO₂ from a new hydrogen plant is estimated at 12 \$/tCO₂, which can be compared to 44 \$/tCO₂ for a new natural gas combined cycle plant (36, Table 8.1).²¹

Conclusions

The CO₂ emissions from oil shale production are dependent on properties of both the shale itself and the retorting process used. Important shale properties

²¹ These are 2002 dollars. These estimates are deemed representative values, with ranges of 2-39 \$/tCO₂ for the hydrogen plant and 33-57 \$/tCO₂ for the NGCC plant.

include the fraction organic matter, the mineral makeup of the shale, and the raw shale moisture content. The key retorting properties affecting CO₂ emissions are the retorting temperature and residence time, as well as the amount of heat recovery from spent shale.

The industry-scale model of CO₂ emissions described here is intended to highlight the value of transparent, mechanistic and probabilistic modeling tools to estimate the potential emissions and to define the most significant parameters. This will focus research efforts by allowing improvements to those model components that are most likely to affect the outcome. Further refinement of this model is necessary to more accurately reflect the expected CO₂ release from an in situ oil shale industry.

This simple model suggests that the dominant CO₂ source would most likely be power plant emissions. Refinement of the model is likely to further strengthen this conclusion. Concern about the amount of CO₂ produced with the gaseous fraction is reasonable. It will be important to better define sources of CO₂ from underground, both organic and mineral in nature. It is possible that such refinements will demonstrate that a small percentage of the rock mass is reacted, thereby reducing the fraction of CO₂ from underground sources.

Collected estimates from a variety of sources, based on both operating data and models of production processes, suggest that, without mitigation, full-fuel-cycle emissions from the production, refining, and consumption of refined fuels from oil shale (in this case reformulated gasoline) will result in CO₂ emissions that are approximately 1.25 to 1.75 times those from conventional petroleum production.

These baseline emissions can be lowered with a variety of mitigation options, including fuel switching, efficiency improvements, and carbon capture and sequestration. As many of these mitigation technologies are untried, there is still uncertainty about which option will be most cost effective. But, there is little doubt that CO₂ mitigation from oil shale production will be required if greenhouse gas regulations become binding.

Works cited

1. Dyni, J. R. *Geology and resources of some world oil-shale deposits*; 2005-5294; US Geological Survey: Reston, Virginia, 2006; p 42.
2. Boak, J., *Proceedings of the 26th oil shale symposium*. Colorado School of Mines: Golden, CO, 2007, Colorado Energy Research Institute Document 2007-3.
3. Sundquist, E. T.; Miller, G. A., Oil shales and carbon dioxide. *Science* **1980**, 208 (4445), 740-741.

4. Boak, J., CO₂ release from in-situ production of shale oil from the Green River formation in the western United States. In *27th Oil Shale Symposium*, Boak, J., Ed. Colorado School of Mines: Golden, CO, 2008, Colorado Energy Research Institute Document 2008-1.
5. Brandt, A. R., Comparing the Alberta Taciuk Processor and the Shell In Situ Conversion Process - Energy inputs and greenhouse gas emissions. In *27th Oil Shale Symposium*, Boak, J., Ed. Colorado School of Mines, Golden CO, 2008, Colorado Energy Research Institute Document 2008-1.
6. Brandt, A. R., Converting oil shale to liquid fuels: Energy inputs and greenhouse gas emissions of the Shell in situ conversion process. *Environ. Sci. Technol.* **2008**, 42 (19), 7489-7495.
7. Burnham, A. K.; Carroll, S., CO₂ sequestration in spent oil shale retorts. In *28th Oil Shale Symposium*, Boak, J., Ed. Colorado School of Mines, Golden CO, 2009, Colorado Energy Research Institute Document 2009-2.
8. Burnham, A. K.; McConaghy, J. R. *Comparison of the acceptability of various oil shale processes*; UCRL-CONF-226717; Lawrence Livermore National Laboratory: Livermore, CA, 2006.
9. Friedmann, S. J. In *In-situ oil-shale recovery, carbon capture and storage, and the importance of large projects*, 26th Oil Shale Symposium, Colorado School of Mines, Golden CO, Boak, J., Ed. 2007, Colorado Energy Research Institute Document 2007-3.
10. Hatfield, K. E.; Smoot, L. D.; Coates, R. L., Near-zero CO₂ emissions from the clean, shale-oil surface (C-SOS) process. In *28th Oil Shale Symposium*, Colorado School of Mines, 2008.
11. Hendrickson, T. A., *Synthetic fuels data handbook*. Cameron Engineers, Inc.: 1975.
12. Lee, S.; Speight, J. G.; Loyalka, S., *Handbook of alternative fuel technologies*. CRC Press: Boca Raton, FL, 2008.
13. Camp, D. W., Oil shale heat capacity relations and heats of pyrolysis and dehydration. In *Twentieth Oil Shale Symposium*, Gary, J. H., Ed. Colorado School of Mines Press: Colorado School of Mines, 1987; pp 130-144.
14. Burnham, A. K. *Chemical kinetics and oil shale process design*; UCRL-JC-114129; Lawrence Livermore National Laboratory: Livermore, CA, July, 1993.
15. Mraw, S. C.; Keweshan, C. F., Calorimetric determination of the heat of retorting oil shales to 773 K. *Fuel* **1986**, 65 (1), 54-57.
16. Campbell, J. H. *The kinetics of decomposition of Colorado oil shale II: carbonate minerals*; Lawrence Livermore National Laboratory: Livermore, CA, March 13, 1978.
17. Burnham, A. K.; Kirkman Bey, N.; Koskinas, G. J., Hydrogen sulfide evolution from Colorado oil shale. In *Oil shale, tar sands, and related materials*, Stauffer, H. C., Ed. American Chemical Society: 1980.

18. Burnham, A. K.; Taylor, R. W. *Occurrence and reactions of oil shale sulfur*; UCRL-87052; Lawrence Livermore National Laboratory: Livermore, CA, 1982.
19. Thorsness, C. B. *Modeling study of carbonate decomposition in LLNL's 4TU pilot oil shale retort*; Lawrence Livermore National Laboratory: Livermore, CA, October 14, 1994.
20. Taciuk, W.; Caple, R.; Goodwin, S.; Taciuk, G. Dry thermal processor. US patent number 5217578. 1993.
21. Speight, J. G., *Fuel science and technology handbook*. Marcel Dekker: New York, 1990.
22. EIA *Carbon emissions factors - per quadrillion (10¹⁵) BTU*; Energy Information Administration: Washington, D.C., Accessed March 2009, 2009.
23. Huss, E. B.; Burnham, A. K., Gas evolution during pyrolysis of various Colorado oil shales. *Fuel* **1981**, *61* (December), 1188-1196.
24. EIA *Electric power annual 2007*; Energy Information Administration: Washington, D.C., 2009.
25. OSEC *Oil shale research, development, and demonstration project: White River mine, Uintah County, Utah*; Oil Sands Exploration Company and U.S. Department of the Interior, Bureau of Land Management, Vernal field office: Vernal Utah, September 18, 2006.
26. SPP *Stuart oil shale project - Stage 2 consolidated report*; Queensland Government, Department of Infrastructure and Planning: November, 2003.
27. Stanfield, K. E. *Properties of Colorado oil shale*; U.S. Bureau of Mines: 1951.
28. Campbell, J. H.; Gallegos, G.; Gregg, G., Gas evolution during oil shale pyrolysis 2: kinetic and stoichiometric analysis. *Fuel* **1980**, *59* (October), 727-732.
29. IPCC *Good Practice Guidance and Uncertainty Management in National Greenhouse Gas Inventories*; IPCC XVI/Doc. 10 (1.IV.2000); Intergovernmental Panel on Climate Change: Montreal, May, 2000.
30. Singleton, M. F.; Koskinas, G. H.; Burnham, A. K.; Ralyey, J. H. *Assay products from green river oil shale*; UCRL-53272, Rev. 1; Lawrence Livermore National Laboratory: Livermore, CA, February 18, 1986.
31. Jukkola, E. E.; Denilauler, A. J.; Jensen, H. B.; Barnet, W. I.; Murphy, W. I. R., Thermal decomposition rates of carbonates in oil shale. *Industrial and Engineering Chemistry* **1953**, *45* (12), 2711-2714.
32. Probst, R. F.; Hicks, R. E., *Synthetic fuels*. Dover Publications: Mineola, NY, 2006.
33. Speight, J. G., *Synthetic fuels handbook: properties, process, and performance*. McGraw Hill: New York, 2008.

34. Berchenko, I.; Rouffignac, E. P.; Fowler, T. D.; Karanikas, J. M.; Ryan, R. C.; Shahin, G. T.; Stegemeier, G. L.; Vinegar, H. J.; Wellington, S. L.; Zhang, E. *In situ thermal processing of an oil shale formation using a pattern of heat sources*; 6991032 B2; Shell Oil Company: 2006.
35. Johnson, H. R.; Crawford, P. M.; Bunger, J. W. *Strategic significance of America's oil shale resource: Volume II - oil shale resources, technology and economics*; AOC Petroleum Support Services, LLC: Washington, D.C., March, 2004.
36. IPCC, *Special report on carbon dioxide capture and storage*. Cambridge University Press: Cambridge, UK, 2005.
37. Wang, M. Q. *Estimation of energy efficiencies of U.S. petroleum refineries*; Center for Transportation Research, Argonne National Laboratory: Argonne, IL, March, 2008.
38. Wang, M.; Lee, H.; Molburg, J., Allocation of energy use in petroleum refineries to petroleum products - Implications for life-cycle energy use and emission inventory of petroleum transportation fuels. *Int. J. Life Cycle Assess.* **2004**, 9 (1), 34-44.
39. ISO, ISO 14044: Environmental management - Life cycle assessment - Requirements and guidelines. ISO: Geneva, 2006.
40. EIA *Natural Gas 1998 - Issues and Trends*; Energy Information Administration: Washington, D.C., 1999.
41. Burnham, A. K.; McConaghy, J. R., Comparison of the acceptability of various oil shale processes. In *26th Oil Shale Symposium*, Golden CO, 2007, Colorado Energy Research Institute Document 2007-3.
42. Yamada, S.; Koga, N., Kinetics of the thermal decomposition of sodium hydrogencarbonate evaluated by controlled rate evolved gas analysis coupled with thermogravimetry. *Thermochim. Acta* **2005**, 431, 38-43.
43. Campbell, J. H. *Modified in situ retorting: Results from LLNL pilot retorting experiments*; Lawrence Livermore National Laboratory: Livermore, CA, 1981.
44. Baughman, G. L., *Synthetic fuels data handbook, Second edition*. Cameron Engineers: Denver, CO, 1981.
45. Vinegar, H., Shell's In-situ Conversion Process. In *26th Oil Shale Symposium*, Boak, J., Ed. Colorado School of Mines: Golden CO, 2007; Colorado Energy Research Institute Document 2007-3.
46. Wang, M. Q. *GREET Model 1.8b*; Argonne National Laboratory: Available from <http://www.transportation.anl.gov/software/GREET/>, 2008.
47. Charpentier, A. D.; Bergerson, J.; MacLean, H. L., Understanding the Canadian oil sands industry's greenhouse gas emissions. *Environmental Research Letters* **2009**, 4 (014005), 14.

48. Wikipedia List of countries by carbon dioxide emissions. http://en.wikipedia.org/wiki/List_of_countries_by_carbon_dioxide_emissions.
49. Elvidge, C. D.; Erwin, E. H.; Baugh, K. E.; Tuttle, B. T.; Howard, A. T.; Pack, D. W.; Milesi, C., Satellite data estimate worldwide flared gas volumes. *Oil Gas J.* **2007**, (November 12), 50-58.
50. Bridges, J. E., Wind power energy storage for in situ shale oil recovery with minimal CO₂ emissions. *IEEE Transactions on Energy Conversions* **2007**, 22 (1), 103-109.
51. Forsberg, C., Nuclear energy for a low-carbon-dioxide-emission transportation system with liquid fuels. *Nuclear technology* **2008**, 164 (December), 348-367.
52. Berger, R.; Fletcher, E. A., Extracting oil from shale using solar energy. *Energy* **1988**, 13 (1), 13-23.
53. Burnham, A. K., On solar thermal processing and retorting of oil shale. *Energy* **1989**, 14 (10), 667-674.
54. Lerwick, P.; Vawter, G.; Day, R.; Harris, H. G., The EGL oil shale process. In *26th Oil Shale Symposium*, Boak, J., Ed. Colorado School of Mines, Golden CO, 2007, Colorado Energy Research Institute Document 2007-3.
55. DOE *Secure fuels from domestic resources: the continuing evolution of America's oil shale and tar sands industries*; U.S. Department of Energy, Office of Petroleum Reserves, Office of Naval Petroleum and Oil Shale Reserves: Washington, D.C., June, 2007.
56. Day, R.; P., L.; Burnham, A. K.; Vawter, G.; Wallman, H.; Harris, G.; Hardy, M., The EGL Oil Shale Project. In *27th Oil Shale Symposium*, Boak, J., Ed. Colorado School of Mines, Golden CO, 2008, Colorado Energy Research Institute Document 2008-1.
57. Brandt, A. R. *Converting Green River oil shale to synthetic crude oil with the ATP retort: Energy inputs and greenhouse gas emissions*; Energy and Resources Group, University of California: Berkeley, CA, June 1, 2007.
58. Rojek, L. *Personal communication with L. Rojek regarding ATP reactor*; September, 2008.